

Design of multiband isotropic ultrahigh refractive index metamaterials in the terahertz region

BO FANG^{a,b}, YUJIE CHEN^a, CHENXIA LI^a, XUFENG JING^{a,*},

^aChina Jiliang University, Hangzhou 310018, China

^bUniversity of Shanghai for Science and Technology, No. 516 JungGong Road, Shanghai 200093, China

A extremely high refractive index metamaterial can be realized by decreasing the diamagnetic effect in metallic unit and increasing the effective permittivity through strong capacitive coupling. Based on design of a square-shaped metallic patches metamaterial, the peak index of refraction near 33.5 at 0.9THz can be achieved. When the second square-shaped patch is nested in metamaterial, a dual band high refractive index is achieved. Both of the high index bands can separately correspond to different component in metamaterial structure. Then, a triple nested square-shaped metallic patches metamaterial to realize multiband high refractive index performance was designed.

(Received August 11, 2017)

Keywords: Metamaterial, High refractive index, Terahertz

1. Introduction

Recently, more attention has been paid to controlling arbitrarily electromagnetic wave, which was realized by the advent of metamaterials [1-6]. Most of previous research on metamaterials focused on achieving the negative refractive index rather than high refractive index [7, 8]. However, ultra-high refractive index of material can provide design variously for the transformation optics [8]. Thus, expanding the high refractive index will launch the scope of spectral research of refractive index material [9]. Previous work on improving the refractive index of the metamaterial by designing metamaterials frequently in atoms [10], or split-ring resonator [11]. Recently, Shin *et al.* has designed a three-dimensional cubic metamaterial to weak the current loops to decrease the diamagnetic effect, leading to high index material [12]. Choi *et al.* designed and fabricated an "T"-shaped terahertz metamaterial with unnaturally high refractive index [13, 14]. Although some high refractive index metamaterials have been designed and fabricated, most of designed metamaterials focused on single frequency band.

In this paper, we designed a multiband metamaterial with high refractive index in terahertz regime on the basis of square-shaped metallic ring on a substrate. Large effective permittivity and permeability of designed metamaterial can be easily achieved. Based on design of a square-shaped metallic patches metamaterial, the peak index of refraction near 33.5 at 0.9THz can be achieved. When the second square-shaped patch is nested in metamaterial, a dual band high refractive index is achieved. By optimizing geometrical parameters of the metamaterials in multi-ring structure, the multiband high refractive index

performance can be obtained.

2. Principle of high refractive index

According to Maxwell's equations, the effective refractive index is determined by effective permittivity and the effective permeability ($n = \sqrt{\mu\epsilon}$). The high dielectric effective permittivity can be achieved by the electrical resonance generated from the capacitive response [13]. Shin pointed out that different aspects of structure can determine their effective permeability and effective permittivity [12]. The capacitive response referring to effective permittivity can be enhanced by reducing the gap width between the metal elements. By decreasing the thickness of the metal elements, a higher effective permeability can be achieved.

Recently, Choi *et al.* proposed a parallel line charge accumulation model to estimate the effective refractive index of metamaterials [14]. The accumulated charges and the scaling of the effective permittivity depended on the gap width between elements. In strongly coupled regime, the accumulated charges were proportional to $L^3 g^{-1}$, and they can be represented as [14]

$$Q \propto \epsilon_0 \epsilon_p \frac{L^3}{g} E_{in}, \quad (1)$$

where ϵ_p is the relative permittivity of the substrate material, L is the length of the unit cell of metamaterial, g is the gap width between metal elements, and E_{in} is the incident electric field. By calculating the amount of the accumulated charges on the line capacitor in the unit cell of

the metamaterial, the effective permittivity of the metamaterial can be estimated by

$$\varepsilon_r = \varepsilon_p + \frac{P}{\varepsilon_0 E}, \quad (2)$$

where P is the polarization density, and it can be approximated by dipole moment per unit volume as

$$P = \frac{Q(L-g)}{L^2 d}. \quad (3)$$

Here, d is the physical thickness of the unit cell of the metamaterial. In Eq. (2), $E = (L/g)^\beta E_{in}$, where β is a dimensionless fitting parameter. Then, the accumulated charges in Eq. (1) are inversely proportional to the gap width of the metallic patch capacitors. The empirical asymptotic formula to the effective refractive index can be obtained with the assumption of effective permeability being unity as [9]

$$n \cong n_p \alpha^{1/2} d^{-1/2} L^{(2-\beta)/2} g^{-(1-\beta)/2}, \quad (4)$$

where α is another dimensionless fitting parameter. As the gap width between metal patches decreases, the capacitive effect becomes dominant, resulting in the index of refraction of the metamaterial being drastically enhanced.

3. Designed metamaterial structure and effective parameters retrieval method

In order to realize a high refractive index performance of metamaterial, the effective permittivity should be drastically increased by strong capacitive coupling through decreasing gap width, and the effective permeability should be enlarged by decreasing the diamagnetic effect with a thin metallic structure element. A single unit cell we designed is shown in Fig. 1. The substrate is of dielectric polyimide material ($n=1.8+0.04i$) with the thickness of $2\mu\text{m}$. The thickness of the square-shaped ring is $0.1\mu\text{m}$ with metal material. The metal used to construct the metamaterials is lossy copper ($\sigma = 5.96 \times 10^7 \text{ S/m}$), and the metallic structure is on the top of substrate.

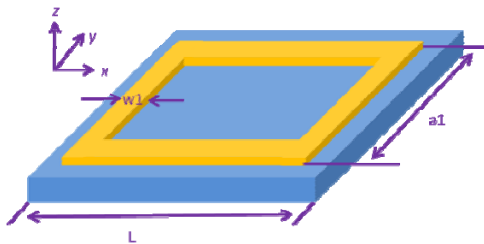


Fig. 1. 3D model of the single band high index metamaterial. The unit cell structure is made of a square-shaped metallic ring patch on dielectric substrate

It is known that in Fig. 1 this metamaterial structure can be equivalent to an homogenous slab under the condition of a long wavelength. The effective constitutive parameters can be obtained by the standard retrieval method of S parameters developed by Smith *et al.* [15-17]. This method to extract the constitutive parameters of metamaterials by using the reflection and transmission coefficients (S parameters) can be applied to numerical simulation and experimental data for the simple and complex structures [18-20].

4. Optimized and calculated results of multiband high refractive index

4.1. Single band metamaterial

Fig. 2 shows the top view schematic, the gap width between the unit cell is defined as $g1=L-a1$, and the width of metallic ring is $w1$. They have a great effect on controlling the effective refractive index of the designed metamaterial. Firstly, the single layer metamaterial with $L=40\mu\text{m}$, $w1=2\mu\text{m}$, $a1=39\mu\text{m}$, $g1=L-a1=1\mu\text{m}$ is determined. Because the square-shaped ring is a centrally symmetrical structure, our designed metamaterial is isotropic with the incident direction of the electric field along x axis.

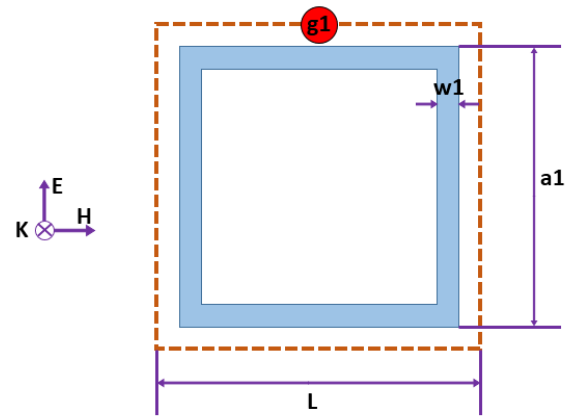


Fig. 2. Top view schematic of the single band high index metamaterial

Fig. 3(a) shows the transmittance and reflectance of the metamaterial with the parameters in Fig. 2 in the THz region. The phase of the calculated S parameters is showed in Fig. 3(b). The effective constitutive parameters of metamaterials can be obtained by the standard retrieval method, the effective permeability, the effective permittivity and the effective refractive index. Based on the transmittance and reflection coefficients and the phase properties in Fig. 3, a peak of effective permittivity about 550 at about 1.0THz can be extracted in Fig. 4(a). These effective permittivities are significantly greater than the effective permittivity of the bare polyimide film [7]. We also get a peak permeability of about 5.1 at about 1.1THz

in Fig. 4(b). It can be revealed that that strong resonant results exist in g_1 , and reducing the gap width can improve the effective permittivity. The thin square-shaped metallic ring structure can effectively decrease the diamagnetic

response to get a high effective permeability. So the peak of effective refractive index achieves about 33 at about 1.0THz in Fig. 4(c).

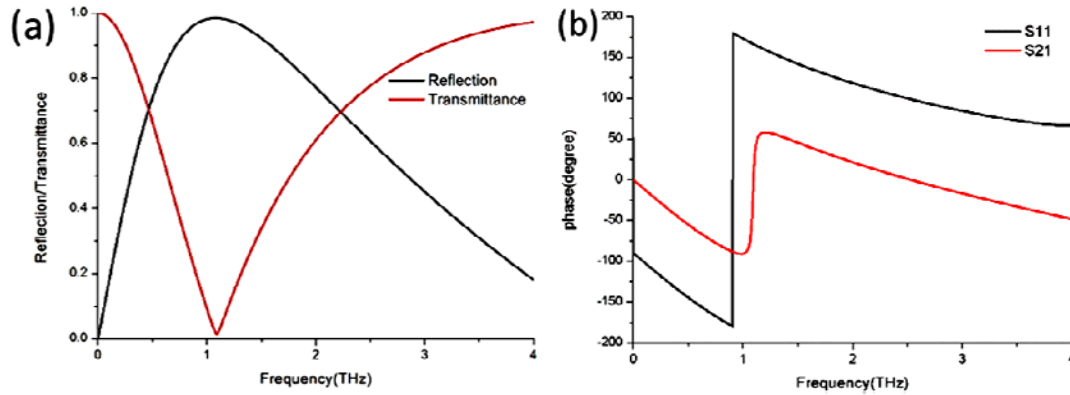


Fig. 3. (a)Transmission/reflection spectra of the single band high index metamaterial.(b)The phase of the caculated S parameters

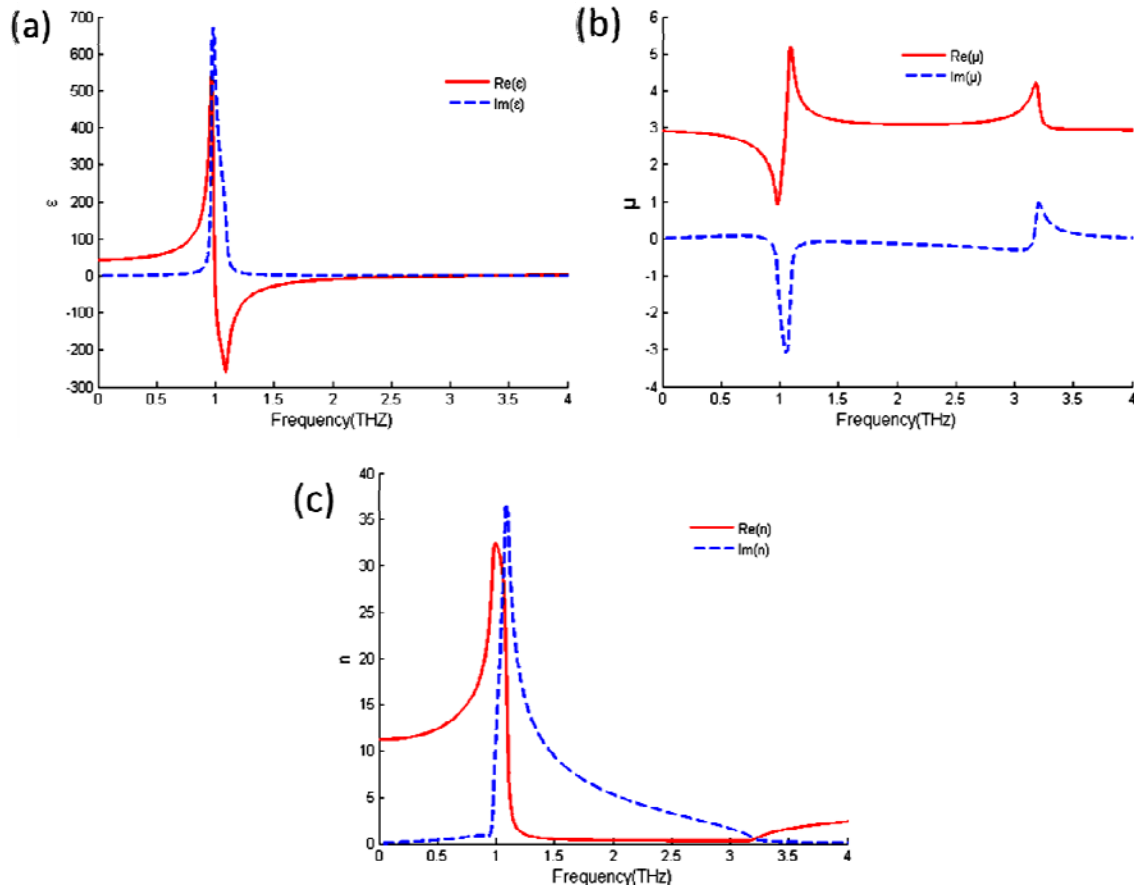


Fig. 4. Extracted effective permittivity (a), permeability (b), refractive index (c) for a single band high index metamaterial with the single-square-shaped metallic ring patches

For obtaining the physical origin of single band high refractive index of the metamaterial, we simulated the electric and magnetic field distribution around the metallic patch between four unit cells at 0.3THz. It can be seen in Fig. 5 that the strong electric field is concentrated in the

gap between unit cells, resulting in the high effective permittivity. And the magnetic field penetrated deeply into the unit cells at 0.3THz, leading to decrease of the diamagnetic effect in metamaterial. These characteristics of the electric and magnetic field distributions are

consistent with the extracted dielectric constant and magnetic permeability.

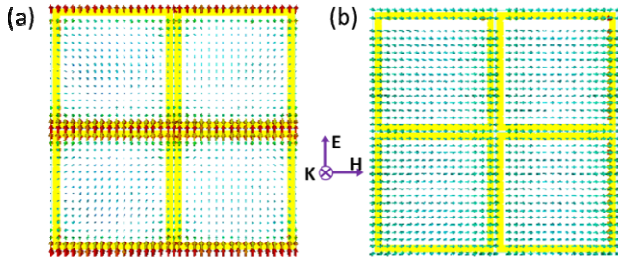


Fig. 5. (a) Saturated electric field distribution at 0.3 THz, (b) the vector plot of the magnetic field distribution at 0.3 THz in the four unit cells

The gap width is a key geometric parameter used to increase the refractive index of the metamaterial. In order to clarify the effect of the gap between unit cells on the effective refractive index, Fig. 6 demonstrates the change of effective refractive index as a function of gap

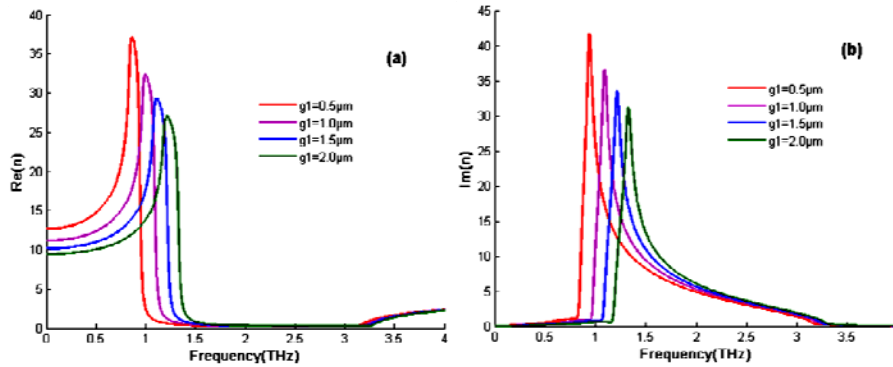


Fig. 6. (a) the real part of the index, and (b) the imaginary part of the index as a function of gap width g_1

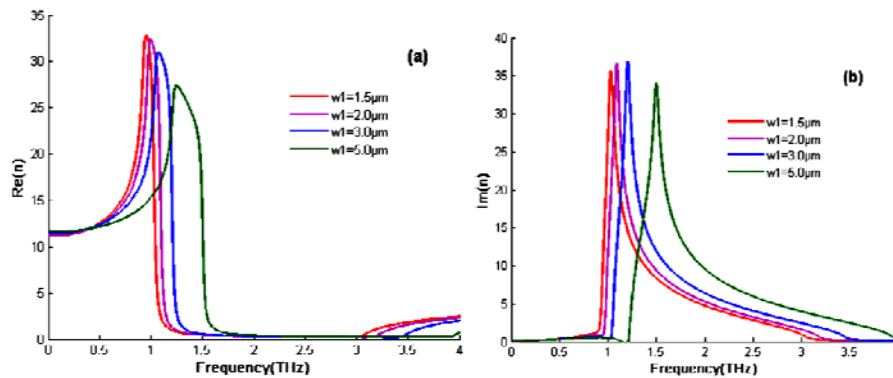


Fig. 7. (a) the real part of the index, and (b) the imaginary part of the index as a function of w_1

4.2. Dual band high index metamaterial

The above design and analysis have indicated that a single band high refractive index can be realized by a single-square-shaped ring. In order to get a multiband refractive Index metamaterial, the second square ring is nested in the middle of the first one to create a

width g_1 with other parameters unchanged. It is found the increase of gap width g_1 makes lower effective refractive index but makes the position of peak value moving to a higher frequency. So, it is expected that one can get arbitrary high refractive index through decrease the width of gap. Moreover, another important factor in increasing the effective refractive index is the metallic beam width, which is related to the diamagnetic response in metamaterial. The dependent effective refractive index on w_1 is demonstrated in Fig. 7. The increase of beam with w_1 results in the reduction of the peak index and the position of the peak index also moves to a higher frequency.

Based on the above analysis about the single band high index metamaterial, it can be seen that both the decrease of gap width and beam width can decrease the current loops and improve the effective refractive index of metamaterial.

double-square-shaped ring metamaterial structure, which is still centrosymmetric, as shown in Fig. 8. Here, the parameters of the unit cell, $L=40\mu\text{m}$, $a_1=39\mu\text{m}$, $a_2=33\mu\text{m}$, $w_1=w_2=2\mu\text{m}$, $g_1=1\mu\text{m}$, $g_2=1\mu\text{m}$, were defined. The gap width, g_1 , is expressed by $g_1=L-a_1$. The second gap width in unit cell, g_2 , is expressed by $g_2=a_1-a_2-2*w_1$.

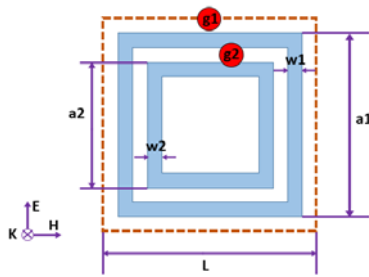


Fig. 8. Schematic of the dual band high index metamaterial. The unit cell structure is made of dual square-shaped metallic patch ring on the dielectric

When the double-square-shaped ring metamaterial structure was exposed to the normal incident THz electromagnetic field, the reflectance and transmittance of the metamaterial were calculated in Fig. 9. The presence of two gaps in the unit cell of designed metamaterial results in a dual band performance, which is different from the single band metamaterial in the refractive index and the transmission spectra. There exist two resonant frequency, one is at frequency of 1.1THz, the other is at 1.8THz. The phase of the structure is indicated in Fig. 9(b).

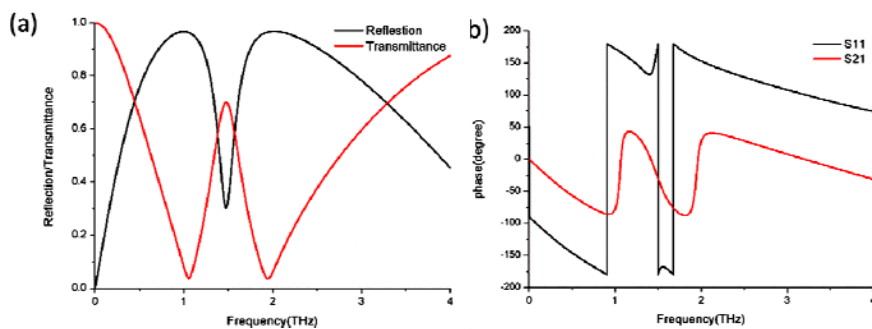


Fig. 9. (a)Transmission/reflection spectra of the dual band high index metamaterial.(b)The phase of the calculated S parameters

The effective permittivity, the effective permeability and the effective refractive index for designed dual band metamaterial can be extracted by S parameters method as shown in Fig. 10. The strong electric resonance is inspected with a peak permittivity of 320 at about 1.1THz, and the weak one appears with the peak permittivity of

about 95 at about 1.7THz. These effective permittivities are also greatly larger than the bare polyimide films[7]. As mentioned in the single structure, it can be deduced that the strong electrical resonance results from the g_1 in the unit cell and the weak electrical resonance is relevant to g_2 .

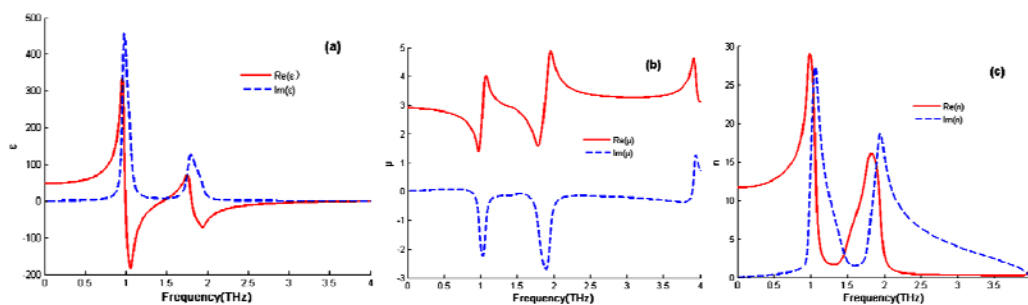


Fig. 10. Extracted effective permittivity, permeability, refractive index for a dual band high index metamaterial with the double-square-shaped metallic ring patches

In order to reveal the physical origin of high refractive index of the metamaterial for the double-ring-shaped structure, the electric and magnetic field were numerically simulated around the metallic patch at the frequency of 0.3THz. In Fig. 11(a), the electric field is strongly concentrated in the gaps between unit cells and between

rings, resulting in a dual band greater effective permittivity. Obviously, the field intensity between rings is slightly weaker than that between unit cells, leading to the larger effective permittivity in the first high refractive index band referring to g_1 . In Fig. 11(b), due to the negligible metal volume fraction corresponding to the current loop with the

thin metallic rings, the magnetic field penetrates deeply into the unit cell. So the designed double-square-shaped rings can effectively suppress the diamagnetic response, realizing a dual band high refractive index metamaterial.

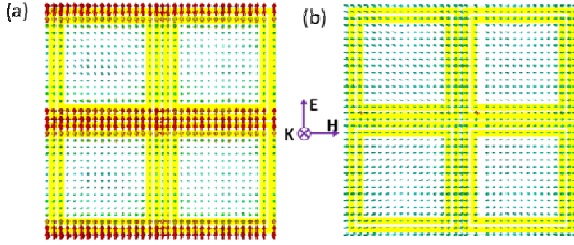


Fig. 11. (a) Sarutated electric field distribution at 0.3THz, (b) the vector plot of the magnetic field distribution at 0.3 THz in four unit cells

After optimizing the parameters of component in unit cell, it can be seen that the peak of first band is higher when compared with that of first band, as shown in Fig. 12. It is found that the effective refractive index peak for second high index band has a blue-shift with the increase of gap width g_2 . It can be attributed to the capacitive response of the gap width g_2 and the decrease of polarization density. The first peak of high refractive index can be attributed to the gap width g_1 . In Fig. 12, with the increase of w_2 and $g_2=2$, the effective refractive index of the second band also have a blue-shift. But the effective refractive index of the first band is not slightly changed when g_2 and w_2 are changed. Above all, it can be easily predicted the dependence of the first high refractive index band depends on gap width g_1 , and the gap width g_2 has greatly influence on the second high refractive index band.

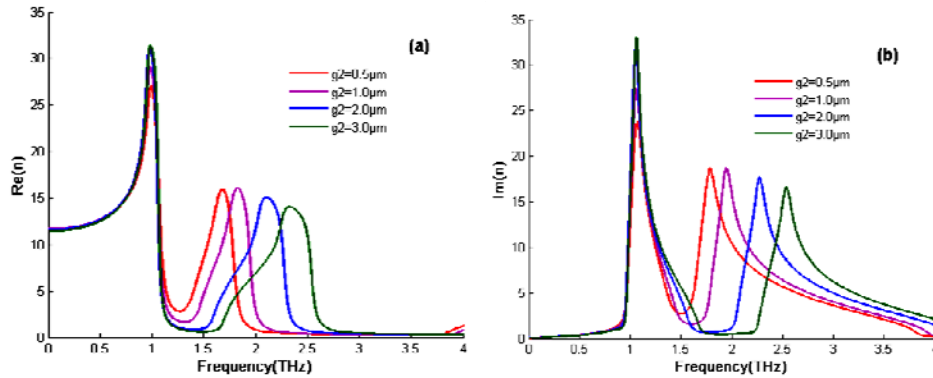


Fig. 12. Gap width of g_2 dependent effective refractive index: (a) the real part of the index, and (b) the imaginary part of the index

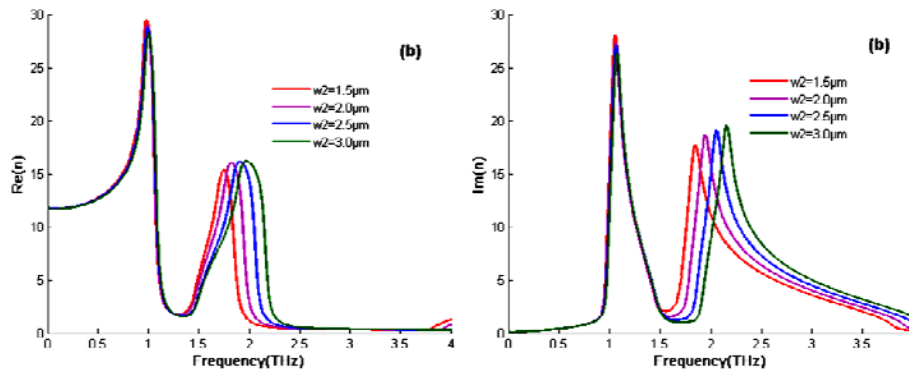


Fig. 13. Effective refractive index as a function of w_1 , (a) the real part of the index, and (b) the imaginary part of the index

4.3. Triple band metamaterial

As shown in Fig. 14, the third square ring is nested into the pervious structure to create a triple-square-shaped metamaterial structure. The parameters of the unit cell, $L=40\mu\text{m}$, $a_1=39\mu\text{m}$, $a_2=33\mu\text{m}$, $a_3=25\mu\text{m}$, $w_1=w_2=2\mu\text{m}$, are defined. The gap width g_3 , is expressed by $g_3=a_2-a_1-2*w_2$. After optimizing the parameters of

component in the unit cells, g_3 and w_3 , as shown in Fig. 15. As the gap width g_3 increased, the peak of the first high index band is slightly enhanced, the peak of the third high index band have a blue-shift with a slight decline. When the beam width w_3 is increased, the peak of the third high index band also have a blue-shift with a slight decline, however, the peaks of the first and the second high index band almost are unaffected. It can be easily

predicted that a triple band high effective refractive index metamaterial can be achieved by selecting a suitable gap width g_3 and decreasing the beam width of w_3 .

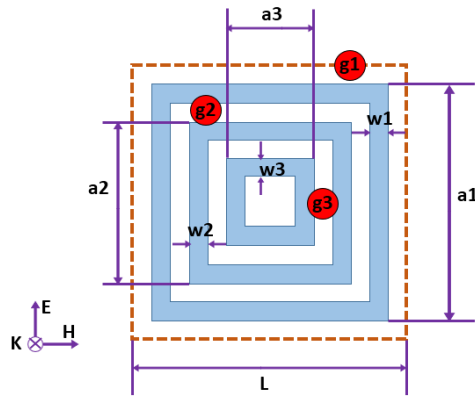


Fig. 14. Schematic of the triple band high index metamaterial

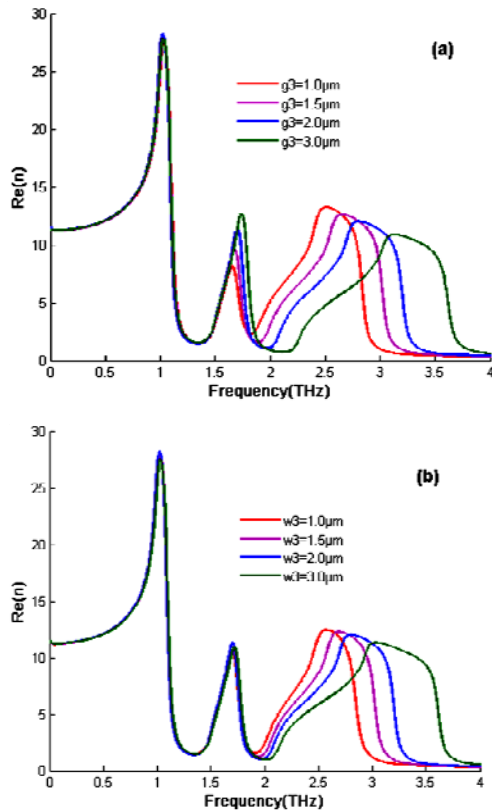


Fig. 15. (a) Gap width of g_3 dependent effective refractive index: the real part of the index, (b) effective refractive index on w_1 : the real part of the index

In order to demonstrate the physical origin of the triple band high refractive index, the electric field and magnetic field distribution at 0.3 THz were calculated numerically in four unit cells in Fig. 16. In Fig. 16(a), the strong electric field is concentrated in the gap between the square rings. And due to the negligible metal volume fraction corresponding to the current loop, the magnetic field penetrates deeply into the unit cells at 0.3 THz.

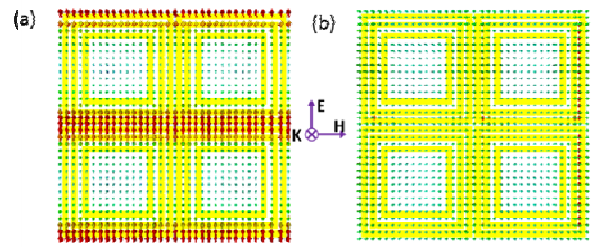


Fig. 16. (a) Saturated electric field distribution at 0.3 THz, (b) the vector plot of the magnetic field distribution at 0.3 THz in the unit cells

5. Conclusions

In summary, the artificial multiband isotropic high refractive index metamaterial in the terahertz region can be achieved by several square metallic ring patches. The obtained dependence of the triple band effective refractive index on the geometric parameters provides a guidance for designing multiband high index metamaterials and experimental investigation and broaden the application field of metamaterial, such as wide-angle metamaterial lens, lithography and cloaking devices.

Acknowledgements

The authors acknowledge the support from the National Key Research and Development Plan (Grant No. 2016YFF0100505), National Program on Key Basic Research Project of China (973 Program) (2014CB339806), Shanghai leading talent (2016-2019), and Young Yangtse Rive Scholar.

References

- [1] D. Schurig, J. Mock, B. Justice, S. Cummer, J. Pendry, A. Starr, Metamaterial Electromagnetic Cloak at Microwave Frequencies. *Science* **314**(5801), 977 (2006).
- [2] W. Wang, F. Yan, S. Tan, H. Zhou, Y. Hou, *Photonics Research* **5**(6), 571 (2017).
- [3] X. Jing, X. C. Gui, R. Xia, Z. Hong, *IEEE Photonics Journal* **9**(1), 5900107, (2017).
- [4] D. Sun, M. Wang, Y. Huang, Y. Zhou, M. Qi, M. Jiang, Z. Ren, *Chinese Optics Letters* **15**(5), 051603 (2017).
- [5] W. Zhu, M. Jiang, H. Guan, J. Yu, H. Lu, J. Zhang, Z. Chen, *Photonics Research* **5**(6), 684 (2017).
- [6] Lawrence R. Chen, *Chinese Optics Letters* **15**(1), 010004 (2017).
- [7] Z. Yang, F. Gao, Y. Hou, D. Hu, L. Pang, X. Wu, *Chin. Opt. Lett.* **14**, 061602 (2016).
- [8] R. Liu, C. Ji, J. Mock, J. Chin, T. Cui, D. Smith, *Science* **323**(5912), 366 (2009).

- [9] X. Jing, W. Wang, R. Xia, J. Zhao, Y. Tian, Z. Hong, *Appl. Opt.* **55**(31), 8743 (2016).
- [10] M. O. Scully, *Phys. Rev. Lett.* **67**(14), 1855 (1991).
- [11] J. B. Pendry, A. J. Holden, D. J. Robbins, W. J. Stewart, *IEEE Transactions on Microwave Theory & Techniques* **47**(11), 2075 (1999).
- [12] J. Shin, J. T. Shen, S. Fan, *Phys. Rev. Lett.* **102**(9), 093903 (2008).
- [13] D. Sievenpiper, E. Yablonovitch, J. Winn, S. Fan, P. Villeneuve, J. Joannopoulos, *Phys. Rev. Lett.* **80**(13), 2829 (1998).
- [14] M. Choi, S. Lee, Y. Kim, S. Kang, J. Shin, H. Min, *Nature* **470**(7334), 369 (2011).
- [15] D. Smith, D. Vier, T. Koschny, C. Soukoulis, *Phys. Rev. E* **71**, 036617 (2005).
- [16] T. Koschny, P. Markos, E. Economou, D. Smith, *Phys. Rev. B* **71**(24), 245105 (2005).
- [17] X. Chen, T. Grzegorzczak, B. Wu, J. Pacheco, J. Kong, *Phys. Rev. E* **70**(1), 016608 (2004).
- [18] Gil Litmanovitch, D. Rrotshild, A. Abramovich, *Chinese Optics Letters* **15**(1), 011101 (2017).
- [19] Luigi Bibbò, Karim Khan, Qiang Liu, Mi Lin, Qiong Wang, Zhengbiao Ouyang, *Photonics Research* **5**(5), 500 (2017).
- [20] Zhengyuan Bai, Guiju Tao, Yuanxin Li, Jin He, Kangpeng Wang, Gaozhong Wang, Xiongwei Jiang, Jun Wang, Werner Blau, Long Zhang, *Photonics Research* **5**(4), 280 (2017).

*Corresponding author: jingxufeng@cjlu.edu.cn